Journal of Engineering Science and Technology
Vol. 13, No. 12 (2018) 3995 - 4009

METHODS FOR OPTIMAL CONTROL OF GRINDING PROCESSING ACCURACY ON LOW RIGIDITY SHAFTS

B. M. AZIMOV, L. F. SULYUKOVA*

Scientific and Innovation Center of Information and Communication Technologies under
IT University, Kichik halka yuli st., 2, Tashkent, Uzbekistan
*Corresponding Author: slf72@yandex.com

Abstract

This article addresses the application of modern methods and algorithms for the optimal control of technological processes and the efficient design of grinding process for low rigidity shafts. The investigation of the dynamic processing characteristics of the system identifies the influence of disturbing and regulatory influences on the amount of elastic deformation of the details in the transient and steady modes in order to minimize shape error of the shafts. The necessary conditions for optimal control of the technological systems under consideration are investigated using the Pontryagin maximum principle. The components of the cutting forces and the optimal values of the geometric, structural and functional parameters of the work-in-process parts are determined.

Keywords: Grinding, Low rigidity shaft, Mathematical modelling Optimal control, Technological process.

1. Introduction

The investigation of the whole process of the outside grinding of round surfaces allows the detection of conditions for avoiding or mitigating negative influences in the quality of the processed surface. Particularly, it refers to investigations with a simulation of a surface grinding process, such as fluctuations from the surroundings, undulations, etc. The most important aspect of these investigations is the possibility to observe grinding transient processes and dynamic effects of the whole operation cycle, and modeling them allows finding the analytical aspects for all of its stages and the choosing of the rational structure and parameters. The purpose of this work is to develop the methods and algorithms for the control of accuracy in the rough grinding of shafts of low rigidity. The control criterion is the optimal operating speed to achieve transient processes control and to provide a productive technological process with an increase in the declared accuracy.

2. Construction of the Kinematic Scheme and Dynamic Models

Grinding is used for treatment of various external cylindrical shapes, flat surfaces and also holes. Grinding of external cylindrical surfaces is the most common case, which is most often done on round grinding machines. The kinematic scheme and dynamic model of grinding is shown on the Fig. 1: here is the grinding cycle 1 goes round at high speed, and the processable roll 2 goes round with speed less than the grinding cycle speed 60-100 times [1-3].

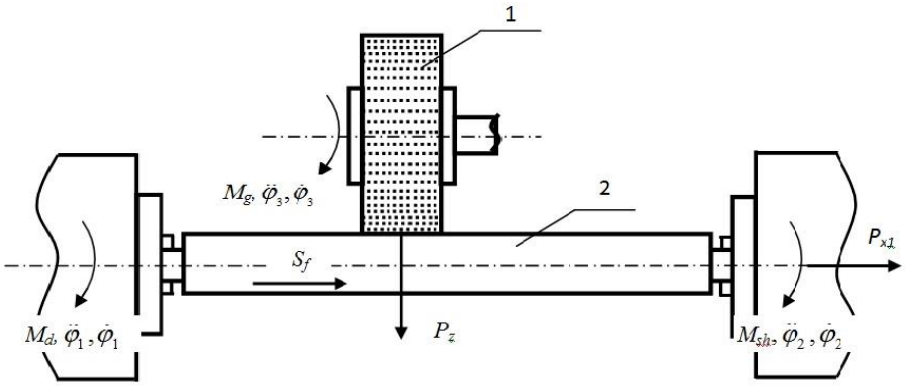

Fig. 1. Kinematic scheme of the round outside *grinding:* 1- grinder; 2 - processable shaft.

To meet the goal objective using the second kind Lagrange equation the mathematic model of the technological system for the rough-grinding processing of small rigidity details was established [4-7].

$$\left.\begin{aligned} j_1\ddot{\phi}_1 &= M_d - b_{sh}(\dot{\phi}_1 - \dot{\phi}_2) - c_{sh}(\phi_1 - \phi_2) \\ j_2\ddot{\phi}_2 &= b_{sh}(\dot{\phi}_1 - \dot{\phi}_2) + c_{sh}(\phi_1 - \phi_2) - M_r \\ j_3\ddot{\phi}_3 &= M_g - M_{sh} \end{aligned}\right\}, \quad (1)$$

where $M_{sh} = j_2\ddot{\phi}_2$, $N{\cdot}m$.

For round outer grinding with longitudinal feed, the roughness parameter Ra=0.4 μm, construction hardened steel HRC45 to accept the grinding wheel with feature 24 A401K, index of grain N, structure 5, class A

According to Zil [3], the total cycle identification is PP24 A40NS15KA - 35 m/s. The grinding wheel dimensions: D_g=600 mm; B_g=63 mm (under the machine chart) [3].

Cutting force (mode of operation)

(i) The grinder speed V_g =35 m/s [3]. Rotation frequency of the grinding wheel head spindle (rev/min)

$$n_g = \frac{1000 \cdot V_g \cdot 60}{\pi \cdot D_g} = \frac{1000 \cdot 35 \cdot 60}{3.14 \cdot 600} = 1114.65 .$$

Correcting under the machine chart, it is established as n_g = 1114 rev/min (it is corrected to a lower value only). Cutting parameters of structural steels supply the final outside round grinding as defined by [3].

(ii) Rotary velocity of a workpiece shaft is accepted as V_{sh}=30 m/min. Rotation frequency of the headstock spindle, correspond to the accepted rotator velocity (rev/min) of the workpiece.

$$n_{sh} = \frac{1000 \cdot V_{sh}}{\pi \cdot d_{sh}} = \frac{1000 \cdot 30}{3.14 \cdot 26} = 367.467 .$$

As rotation frequency of the workpiece is regulated continuously (without steps), it is accepted as n_{sh} = 370 rev/min.

(iii) Grinding depth. Taking into account the stepless regulation of grinding wheel transverse motion on the desk travel, it is accepted as t = 0.005 mm.

(iv) Line feed. It is accepted as $S_f = 0.25 \cdot B_g = 0.25 \cdot 63 = 15.75$ mm/rev.

(v) The velocity of the longitudinal stroke of the table (m/min)

$$V_t = \frac{S_f \cdot n_{sh}}{1000} = \frac{15.75 \cdot 370}{1000} = 5.83$$

Taking into account the machine chart (stepless regulation of the table longitudinal stroke velocity) it is accepted as V_t = 5.8 m/min.

3. Calculation of Cutting Force Components of the Grinding Processing

The cutting force resistance in the cycle grinding process can be resolved into three components: tangential P_z, radial P_y and axial P_x [2, 8-10].

The cutting force component P_z influences the detail curl largely and its value applicable to the rough-grinding process velocity can be defined approximately as [1, 3, 5]:

$$P_z = C_p \cdot V_{sh}^z \cdot S_f^y \cdot t^x \cdot 10 = 2.65 \cdot 30^{0.5} \cdot 15.75^{0.55} \cdot 0.005^{0.5} \cdot 10 = 46.74 \text{ N},$$

where the coefficient C_p depends on the grinding conditions. For tempered steels C_p=2.65 [3].

To determine the forces P_y and P_x there are similar empirical formulas. However, in order to simplify and accelerate the calculations, the values of the forces P_y and P_x are recommended as per the following relations [1, 4-6, 8, 11]:

P_y = (0.25,..., 0.5) P_z, P_x = (0.1, ..., 0.25) P_z,

$$P_y = 0.375 \cdot P_z = 0.375 \cdot 46.74 = 17.53 \text{ N}, \; P_x = 0.175 \cdot P_z = 0.175 \cdot 46.74 = 8.18 \text{ N}.$$

Determining the moment of resistance during the shaft processing

$$M_c = M_z + M_0 \sin \omega t = r_{sh} \cdot P_z + M_0 \sin \omega t = 0.013 \cdot 46.74 + 1.64 \cdot 10^{-9} \sin \omega t =$$
$$= 0.6 + 1.64 \cdot 10^{-9} \sin 38.726 \cdot t,$$

M_0 - mean values of the oscillation amplitude of the resistance moment.

Cutting power

$$N_p = C_p \cdot V_{sh}^z \cdot S_f^t \cdot t^x \cdot d^q = 2.65 \cdot 30^{0.5} \cdot 15.75^{0.55} \cdot 0.005^{0.5} \cdot 0.3^0 = 4.74 \text{ kWt},$$

where d is the diameter of the grinding wheel; x, y, z, q - exponents.

For round external grinding of tempered steel with feeding for each stroke by a grinding wheel with grain 40, hardness CM1 z=0.5; x=0.5; y=0.55; q=0.

By elastic small rigidity details lines model developing and by their processing in the elastic deformed state bending moments on x-axis are taken in to account as more essential qualities, so as elastic deformations on this axis exert dominated influence to form an error in the longitudinal direction.

Azimov and Sulyukova [5, 6] and , Preliminary necessary shaft rigidity in the corresponding moment of resistance is determined.

$$\phi_t = \frac{r_{sh} P_z \cdot l_{sh}}{G \cdot I_p} = \frac{0.013 \cdot 46.74 \cdot 0.95}{8.1 \cdot 10^{10} \cdot 0.1 \cdot (0.026)^4} = 0.000156 \text{ rad},$$

$$\phi_s = \frac{P_y \cdot l_{sh}}{EF \cdot r_{sh}} = \frac{17.53 \cdot 0.95}{2.1 \cdot 10^{11} \cdot \pi \cdot r_{sh}^3} = \frac{17.53 \cdot 0.95}{2.1 \cdot 10^{11} \cdot 3.14 \cdot (0.013)^3} = 0.000011495464422 \text{ rad},$$

$$c_t = \frac{M_R}{\phi_t} = \frac{r_{sh} \cdot P_z}{\phi_t} = \frac{0.013 \cdot 46.74}{0.000156} = 3895 \; \frac{N \cdot m}{\text{rad}},$$

$$c_s = \frac{M_R}{\phi_s} = \frac{r_{sh} \cdot P_z}{\phi_s} = \frac{0.013 \cdot 46.74}{0.000011495464422} = 52857.37 \; \frac{N \cdot m}{\text{rad}},$$

$$P_{x_1} = \frac{c_s \cdot \phi_s}{r_{sh}} = \frac{52857.37 \cdot 0.000011495464422}{0.013} = 46.74 \text{ N}.$$

On the basis of the required rigidity, we determine the corresponding moment of inertia of the processed shaft by solving the conjugate system of the Pontryagin maximum principle.

Further, according to the corresponding shaft parameters, we determine the shaft rigidity and the coefficient of viscous resistance at torsion and stretching:

$$c_{sh} = c_t + c_s = 3895 + 52857.37 = 56752.37 \; \frac{\text{N} \cdot \text{m}}{\text{rad}},$$

$$b_{sh} = \frac{0.64 \cdot c_{sh}}{2\pi\omega} = \frac{0.64 \cdot 41055.4}{2 \cdot 3.14 \cdot 38.726} = 149.35, \frac{\text{Nms}}{\text{rad}}.$$

4. Solution of Optimal Control Problem and Determination of Optimal Parameters of the Shaft Grinding System Functioning

The main purpose of the technological system functional process control is to determine the best transient processes so that the energy, consumed during a transient process was minimum, that is, it is required choosing the control $u(t)$, which transfer the trajectory parameters of a grinding wheel and processable shaft into the target value in the minimum time. Then, the main estimation criteria of the functioning process will be accepted as the periodical operating speed in the form of functional minimizing [5-7, 12-14].

$$J(\phi_0, u(t), \phi(t)) = \int_{t_0}^{T} f^0(\phi(t), u(t), t)dt) \ . \tag{2}$$

At conditions

$$\phi_i(0) = \phi_0(0), \qquad \dot{\phi}_1(0) = \dot{\phi}_0(0). \tag{3}$$

$$\phi_i(t) = \phi_0(t), \qquad \dot{\phi}_1(t) = \dot{\phi}_0(t), \quad 0 \le \mathrm{t} \le \mathrm{T} \quad (i = \overline{1,n}) \tag{4}$$

$$\dot{\boldsymbol{\phi}}(\boldsymbol{t}) = \boldsymbol{f}(\boldsymbol{\phi}(\boldsymbol{t}), \boldsymbol{u}(\boldsymbol{t}), \boldsymbol{t}), \tag{5}$$

$$u \in U, \quad t_0 \le t \le T, \tag{6}$$

where $f(\ldots)$ is continuously differentiable with its derivatives and $u(t)$ is sectional continuous function on an interval $[t_0, T]$.

To research the necessary conditions to the considered technical system optimal control we shall use the maximum principle of Pontryagin [11, 12, 14].

To formulate this maximum principle Hamiltonian and Pontryagin for the technical system is entered into the function

$$H = (\phi, u, t, \psi_i, \psi_0) = -f^0(\phi, u, t) + \langle \psi, u \rangle \tag{7}$$

and conjugate system

$$\left.\begin{aligned} \frac{d\psi_1}{dt} &= -\frac{\partial H_{\mathrm{v}}}{\partial y_1} = -j_2^{-1} c_v \psi_2, \\ \frac{d\psi_2}{dt} &= -\frac{\partial H_{\mathrm{v}}}{\partial y_2} = -\psi_1 + j_2^{-1} b_v \psi_2 \end{aligned}\right\} \tag{8}$$

with limited control $|u| \le 1$.

For problem solving the following condition must be met:

$$H(\phi_i(t), u(t), t, \psi_i, \psi_0) = \max_{u \in U} H(\phi_i(t), u, t, \psi_i(t), \psi_0) \tag{9}$$

Moving to the optimal control determination on the base of Eq. (7), the functions are:

$$\left.\begin{aligned} &\phi_1 = y_1, \ \dot{\phi}_1 = y_2, \ \dot{y}_2 = u_\partial - j_1^{-1}\left[b_v(y_2 - y_4) + c_v(y_1 - y_3)\right] \\ &\phi_2 = y_3, \ \dot{\phi}_1 = y_4, \ \dot{y}_4 = j_2^{-1}\left[b_v(y_2 - y_4) + c_v(y_1 - y_3)\right] - u_c \\ &\phi_3 = y_5, \ \dot{\phi}_5 = y_6, \ \dot{y}_6 = u_\kappa - u_v \end{aligned}\right\} \tag{10}$$

So, if $f^0 \equiv 1$, so $J(\phi_0, u(t), \phi(t)) = T - t_0$. In this case, the task Eqs. (2) to (6) is called the problem of operating speed.

The object under consideration is a stationary system and problem Eq. (4) means that f and U do not depend explicitly on time, i.e.,

$$f(t,y,u) = f(y,u), \quad U(t) = U. \tag{11}$$

If the stationary problem Eqs. (4) and (11) has an optimal control $u(t)$ and an optimal trajectory $\phi_0(t)$ then there exists a nonzero vector $(\psi_1(t), \psi_2(t)), (t) \in R^n$ of conjugate variables satisfying conditions Eq. (9), that is the maximum condition Eq. (7)

$$\psi_0(t) = const \le 0. \tag{12}$$

So as the conjugate system Eq. (8) is congeneric in relation to ψ_i, constant in an equation (12) can be chosen liberally so that

$$\psi_0(t) = -1 \qquad 0 \le t \le T \quad . \tag{13}$$

From the conditions $\max\limits_{|u|<1} H$, it follows $u = sign\psi_2$ at $\psi_2 \neq 0$. Then the boundary problem of the maximum principle will be written as:

$$\left.\begin{aligned} &\phi_1 = y_1,\ \dot{\phi}_1 = y_2,\ \dot{y}_2 = sign\psi_2 - j_1^{-1}\left[b_v(y_2 - y_4) + c_v(y_1 - y_3)\right] \\ &\phi_2 = y_3,\ \dot{\phi}_2 = y_4,\ \dot{y}_4 = j_2^{-1}\left[b_v(y_2 - y_4) + c_v(y_1 - y_3)\right] - sign\psi_2 \\ &\phi_3 = y_5,\ \dot{\phi}_3 = y_6,\ \dot{y}_6 = sign\psi_2 - sign\psi_2 \end{aligned}\right\}. \tag{14}$$

We compose the Hamilton-Pontryagin function, which has the form

$$\left.\begin{aligned} H_1 &= \psi_0 + \psi_1 y_2 + \psi_2 \dot{y}_2 \\ H_2 &= \psi_0 + \psi_1 y_4 + \psi_2 \dot{y}_4 \\ H_3 &= \psi_0 + \psi_1 y_6 + \psi_2 \dot{y}_6 \end{aligned}\right\}. \tag{15}$$

Hence, it is clear that the condition Eq. (9) separates the function $u = sign\psi_2, \quad \psi_2 \neq 0$. The boundary problem Eqs. (10) and (14) consists of

$$H_i = -f^0 u + \psi_2(t) u_\partial \tag{16}$$

In this case

$$u_i = sign\psi_2(t) = \begin{cases} 1, & \psi_2(t) > 1 \\ -1, & \psi_2(t) < 1 \end{cases}, \quad i = 2, 4, \ldots, 2n, \tag{17}$$

i.e., the control $u_k(t)$ can have one switch point only.

5. Discussion of Computing Experimental Results

A conjugate system with a variation of design parameters b_i, c_i, j_i was investigated by a numerical method to determining the conjugate functions (8)

The systems Eqs. (1), (8) and (14) are solved using numerical Runge-Kutts method. Control $u_k(t)$, which gives the maximum of the function Eq. (9), is defined in the domain Eq. (17).

Table 1.The values of velocities, acceleration of transients, obtained by solving the conjugate system and the boundary problem of the Pontryagin maximum principle, for the processed shaft

***T*, s**	$\dot{\phi}_1 \cdot 10^{-3}$, **s^{-1}**	$\ddot{\phi}_1$, **s^{-2}**	$\dot{\phi}_1 \cdot 10^{-3}$, **s^{-1}**	$\ddot{\phi}_1$, **s^{-2}**	$\dot{\phi}_2 \cdot 10^{-3}$, **s^{-1}**	$\ddot{\phi}_2$, **s^{-2}**	$\dot{\phi}_2 \cdot 10^{-3}$, **s^{-1}**	$\ddot{\phi}_2$, **s^{-2}**	$\dot{\phi}_2 \cdot 10^{-3}$, **s^{-1}**	$\ddot{\phi}_2$, **s^{-2}**	$\dot{\phi}_2 \cdot 10^{-3}$, **s^{-1}**	$\ddot{\phi}_2$, **s^{-2}**
	***u*=+1**		***u*=-1**		***u*=+1**		***u*=-1**		***u*=+1**		***u*=-1**	
0	0	1	0	1	0	-1	0	1	0	1	0	-1
0.1	-0.0012	-0.2	0.0012	0.2	-0.0013	0.2	0.0013	-0.2	0.099	1	-0.099	-1
0.2	-0.0023	-0.2	0.0023	0.2	-0.0026	0.2	0.0026	-0.2	0.2	1	-0.2	-1
0.3	-0.0036	-0.2	0.003	0.2	-0.0038	0.2	0.0038	-0.2	0.3	1	-0.3	-1
0.4	-0.0048	-0.2	0.0048	0.2	-0.0052	0.2	0.0052	-0.2	0.4	1	-0.4	-1
0.5	-0.0061	-0.2	0.0061	0.2	-0.0064	0.2	0.0064	-0.2	0.5	1	-0.5	-1
0.6	-0.0074	-0.2	0.0074	0.2	-0.0076	0.2	0.0076	-0.2	0.6	1	-0.6	-1
0.7	-0.0086	-0.2	0.0086	0.2	-0.0088	0.2	0.0088	-0.2	0.7	1	-0.7	-1
0.8	-0.0098	-0.2	0.0098	0.2	-0.01	0.2	0.01	-0.2	0.8	1	-0.8	-1
0.9	-0.0111	-0.2	0.0111	0.2	-0.0113	0.2	0.0113	-0.2	0.9	1	-0.9	-1
1	-0.0123	-0.2	0.0123	0.2	-0.0126	0.2	0.0126	-0.2	1	1	-1	-1

The processing of the results of the solution of system Eq. (8) showed that the change in the moments of inertia and elastic-dissipative forces abrupt changes the function of the variables $\psi_1, \dot{\psi}_1, \psi_2, \dot{\psi}_2$, that is movement of the grinding shaft.

Therefore, to increase the accuracy of the dimensions and shape of the shafts to be processed, it is necessary to determine the variables of the conjugate system, which provided the normal functioning of the TS.

The results of numerical solutions of the system Eq. (1), presented in Tables 1-3 and Figs. 2 and 3, make it possible to determine the following optimal values of the low-rigid shaft grinding parameters, presented in Table 4.

Table 2. The values of velocities, acceleration of the transient processes of the grinding wheel and auxiliary functions of the shaft processing process.

***T*, s**	ψ_1	$\dot{\psi}_1$	ψ_1	$\dot{\psi}_1$	ψ_2	$\dot{\psi}_2$	ψ_2	$\dot{\psi}_2$
	***u*=+1**		***u*=-1**		***u*=+1**		***u*=-1**	
0	0	-1	0	1	0	-1	0	1
0.1	-0.1	-1	0.1	1	-0.1	-1	0.1	1
0.2	-0.2	-1	0.2	1	-0.2	-1	0.2	1
0.3	-0.3	-1	0.3	1	-0.3	-1	0.3	1
0.4	-0.4	-1	0.4	1	-0.4	-1	0.4	1
0.5	-0.5	-1	0.5	1	-0.5	-1	0.5	1
0.6	-0.61	-1	0.61	1	-0.6	-1	0.6	1
0.7	-0.71	-1	0.71	1	-0.7	-1	0.7	1
0.8	-0.82	-1	0.82	1	-0.8	-1	0.8	1
0.9	-0.92	-1	0.92	1	-0.9	-1	0.9	1
1	-1	-1	1	1	-1	-1	1	1

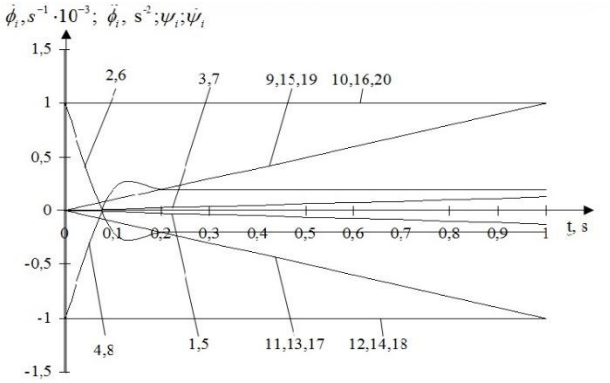

Fig. 2. Graphs of the motion parameters change for the processed shaft and the grinding wheel in the transient process: 1, 5, 9 - angular velocity $\dot{\phi}_1, \dot{\phi}_2, \dot{\phi}_3$, 2, 6, 10 - angular accelerations $\ddot{\phi}_1, \ddot{\phi}_2, \ddot{\phi}_3$ and auxiliary functions 13-ψ_1,14-$\dot{\psi}_1$ 17-ψ_2, 18-$\dot{\psi}_2$ by u(t)= +1; 3-$\dot{\varphi}_1$, 7-$\dot{\phi}_2$, 11-$\dot{\phi}_3$ - angular velocity, 4-$\ddot{\varphi}_1$, 8-$\ddot{\varphi}_2$, 12-$\ddot{\varphi}_3$ - angular accelerations and auxiliary functions - 15-ψ_1,16-$\dot{\psi}_1$ 19-ψ_2, 20-$\dot{\psi}_2$ by u(t)= -1.

Table 3. Parameter of the processing shaft function.

T, s	$\dot{\phi}_1$, s^{-1}	$\ddot{\phi}_1$, s^{-2}	M_d, Nm	$\dot{\phi}_2$, s^{-1}	$\ddot{\phi}_2$, s^{-2}	M_{sh}, Nm	$\dot{\varphi}_3$, s^{-1}	$\ddot{\phi}_3$, s^{-2}	M_g, Nm	n_{sh}, rev/min	n_g, rev/min
0	0	40.47	22.97	0	-60.76	-0.6	0	117.22	66.93	0	0
0.1	3.87	38.33	21.75	3.87	60.49	0.6	11.65	118.33	67.57	36.99	111.34
0.2	7.74	38.33	21.75	7.74	60.48	0.6	23.3	118.33	67.57	73.98	222.68
0.3	11.61	38.33	21.75	11.61	60.52	0.6	34.96	118.33	67.57	110.97	333.98
0.4	15.48	38.33	21.75	15.48	60.48	0.6	46.6	118.33	67.57	147.97	445.15
0.5	19.36	38.33	21.75	19.36	60.38	0.6	58.25	118.33	67.57	184.96	556.52
0.6	23.23	38.33	21.75	23.23	60.38	0.6	69.2	118.33	67.57	221.95	668.01
0.7	27.1	38.33	21.75	27.1	60.38	0.6	81.6	118.33	67.57	258.95	779.54
0.8	30.97	38.33	21.75	30.97	60.38	0.6	93.26	118.33	67.57	295.94	891.06
0.9	34.86	38.33	21.75	34.86	60.53	0.6	104.93	118.33	67.57	333.06	1002.6
1	38.75	38.33	21.75	38.75	60.53	0.6	116.61	118.33	67.57	370.24	1114.11

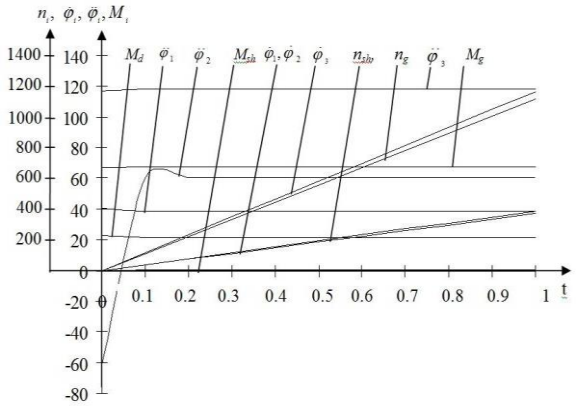

Fig. 3. The characterization of the changing parameters of the TS in the shaft grinding process.

Table 4. Meanings and indexes of in-processing puller shaft geometrical, constructive and functional parameters.

Parameters	Meaning	Index
Geometric dimensions of the in-processing shaft		
Length of the in-processing shaft	950	mm
Diameter of the in-processing shaft	26	mm
Processing conditions:		
Grinder speed -V_g	35	m/s
Rotation frequency of the grinding wheelhead spindle- n_g	1114	rev/min
Rotary velocity of a workpiece shaft - V_{sh}	30	m/min
Rotation frequency of headstock spindle - n_{sh}	370	rev/min
Grinding depth - t	0.005	mm
Line feed - S_f	15.75	mm/rev
Velocity of the longitudinal stroke of the table -V_t	5.8	m/min
Constructive characteristics of the in-processing shaft		
Material - *steel*	35	
Permissible stress by stretching - σ_p	900	kgs/mm^2
Solidity limit -σ	0.35·HB	kgs/mm^2
Total coefficient of the in-processing shaft rigidity - c_{sh}	56752.37	N·m/ rad
Coefficient of the in-processing shaft rolling rigidity -c_t	2799.63	N·m/ rad
Coefficient of the in-processing shaft rigidity by stretching -c_s	52885.514	N·m/ rad
Generalized coefficient of tensile resistance of the shaft - b_{sh}	149.35	N·m·s/ rad
Inertion moment of the headstock- j_1	0. 56752	N·m·s^2
Inertion moment of the tailstock - j_2	0.01	N·m.s^2
Inertion moment of the grinding wheel - j_3	0.571	N·m·s^2
Eccentricity -e	0.001	mm
Parameters of TS functioning		
Driving moment - M_d	22.97	N·m
Driving moment on the grinding wheel - M_g	66.93	N·m
Force in direction of cutting speed - P_z	46.74	N
Resistance moment - $M_z = r_{sh} \cdot P_z$	0.6	N·m
Calculation value of axis stretching force - P_{x1}	46.74	N
Absolute shaft extension by stretching - Δl	$11.49 \cdot 10^{-6}$	m

6. Theoretical Conformities, Deflection and Accuracy

In order to evaluate the possibilities of the method and establish the theoretical regularities of the behavior of the part in longitudinal-transverse bending, the equation of the elastic line of a low-rigid shaft was solved on the basis of the calculation scheme in Fig. 4.

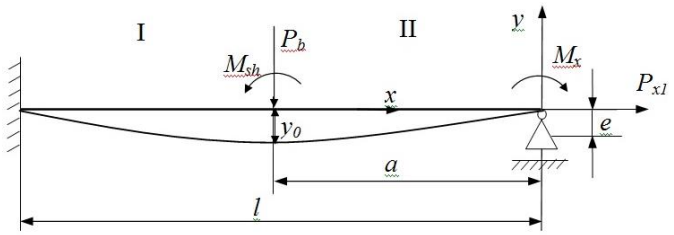

Fig. 4. Calculation scheme of stresses and elastic line of the shaft by stretching: e =0.001- eccentricity of stretching force putting; M_{sh}- cutting forces moment; $M_x=P_{x1}\cdot e$=34.822·0.001=0.034822 Nm -tensile stress moment.

Azimov and Sulyukova [6] commented that description of low rigged shaft elastic line by longitudinal-transverse bend can be represented in the form of fourth order differential equations with the constant coefficients.

$$y_i^4 - k^2 y_i'' = 0 . \tag{18}$$

This equation gives the total elastic line equation for stretching and carrying an arbitrary transverse loading beam

$$y = y_0 + y_0' kx + y_0''(1-\cos kx) + y_0'''(kx - \sin kx) + f(x)$$

where $y_0 = -\dfrac{P_y \cdot l}{48EI}$, y_0', y_0'', y_0''' - accordingly deflection, turn corner, the second and the third derivates in the coordinates beginning; $k = 3...102$ - coefficient determining the details fixing method; *f(x)* - function of transverse loading influence [6].

Elastic line equations on segments I and II (calculation scheme Fig. 4) are

$$\left.\begin{aligned} y_I &= y_0' kx + y_0''(1-\cos kx) + y_0'''(kx - \sin kx) \\ y_{II} &= y_0' kx + y_0''(1-\cos kx) + y_0'''(kx - \sin kx) + f(x) \end{aligned}\right\} \tag{19}$$

The initial parameters are determined by the following:

$$y_0' = -\frac{P_y}{kP_{x1}}\left\{\frac{[kl(\alpha - 1 + \cos\alpha kl) - \sin kl](1-\cos kl)}{kl\cdot\cos kl - \sin kl} - (1-\cos\alpha kl)\right\} + \\ + \frac{M}{P_{x_1}}\left[\frac{(kl\sin kl + \cos kl - 1)(1-\cos kl)}{kl\cos kl - \sin kl} + \sin kl\right],$$

$$y_0''' = \frac{P_y}{kP_{x1}}\left[\frac{kl(\alpha - 1 + \cos\alpha kl) - \sin\alpha kl}{kl\cdot\cos kl - \sin kl}\right] - \frac{M}{P_{x_1}}\left[\frac{kl\sin kl + \cos kl - 1}{kl\cos kl - \sin kl}\right],$$

where $\alpha = \dfrac{l-a}{l}$.

Taking into account that the stretching moment was put at the coordinates beginning it is necessary to determine the initial parameter y_0''. We find it by differentiation of Eq. (19)

$$y_{II}'' = -y_0' k^2 \cos kx - y_0''' k^2 \sin kx . \tag{20}$$

After the multiplication of Eq. (20) to bending and stretching rigidity we will get the equation of bending moment on segment I, taking into account

$$EJ_x = \frac{M_b}{y_2''};\ EF = \frac{M_b \cos\alpha}{y_2''};\ \text{then}$$

$$EI \cdot y_2'' = M_b(x);\ EF \cdot y_2'' = M_b(x) \cdot \cos\alpha. \tag{21}$$

If by x=0, $M_I(0)$=M, so from Eq. (21) is [13]

$$y_0'' = -\frac{P_y \cdot y_2}{EI} + \frac{P_{x_1} \cdot e}{EF},$$

where $y_2 = r_{sh} \cdot \phi_t$.

Take into account the transverse load influence function

$$f(x) = -\frac{P_y(x-a)}{P_{x1}} + \frac{P_y}{kP_{x1}} \sin k(x-a).$$

Finally, deflection equations on the segments will be

$$\left.\begin{aligned} y_I(x) &= -\frac{P_y}{P_{x1}}\left[A(1-\cos kl) - (1-\cos\alpha kl)\right]x + \frac{M}{P_{x1}}[B(1-\cos kl) - \sin kl]kx - \\ &\quad - \frac{M}{P_{x1}}(1-\cos kx) + \left(\frac{P_y \cdot A}{P_{x1}} - \frac{M \cdot B}{P_{x1}}\right)(kx - \sin kx), \\ y_{II}(x) &= y_I(x) - \frac{P_y}{P_{x1}}(x-a) + \frac{P_y}{k \cdot P_{x1}} \sin k(x-a). \end{aligned}\right\}$$

where $A = \frac{kl(\alpha - 1 + \cos\alpha kl) - \sin\alpha kl}{kl\cos kl - \sin kl}$; $B = \frac{kl\sin kl + \cos kl - 1}{kl\cos kl - \sin kl}$.

On the base of the system numerical variables Eq. (1) and calculation scheme, the deflections and puller shaft processing accuracy were calculated and the results are represented in Table 5 and on Fig. 5.

Table 5. The results of calculation of deflections and shaft processing accuracy.

T, s	y_0, µm	y_I, µm	y_{II}, µm	y_{def}, µm
0	-130	3230	3230	3100
0.1	-0.2899	-2.12	-2.12	-2.4
0.2	-0.301	-1.83	-1.83	-2.1
0.3	-0.25	-2.97	-2.97	-3.23
0.4	-0.29	-2	-2	-2.32
0.5	-0.4	0.6	0.6	0.235
0.6	-0.4	0.636	0.636	0.235
0.7	-0.4	0.636	0.636	0.235
0.8	-0.4	0.636	0.636	0.235
0.9	-0.248	-3.166	-3.166	-3.41
1	-0.248	-3.166	-3.166	-3.41

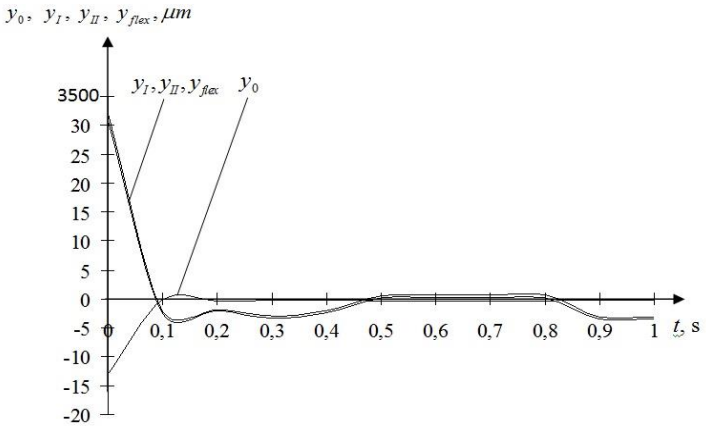

Fig. 5. The functional dependence of accuracy changes for the technological process of shaft grinding.

7. Experimental Researches

To perform empirical studies of the influence of the grinding process with the use of an elastically deformed state of the shaft and with standard grinding on the geometric form accuracy, a circular geometry gage "MMQ 400 CNC" model was used to estimate the form error. The polar-recording charts of details transverse sections were constructed with device. Transverse sections were used as base surfaces.

Analysis of the results on the roundness accuracy of the detail was carried out in five sections. Visualization of the process of the measuring of inaccuracy roundness form is shown in the form of the polar-recording charts in Fig. 6.

The analysis of experimental dependences showed that the value of the axis offsetting in grinding depends on the process character and increases with the occurrence of self-oscillations. With the increase of the bending rigidity of the workpiece the offsetting of the axis decreases and its shape changes.

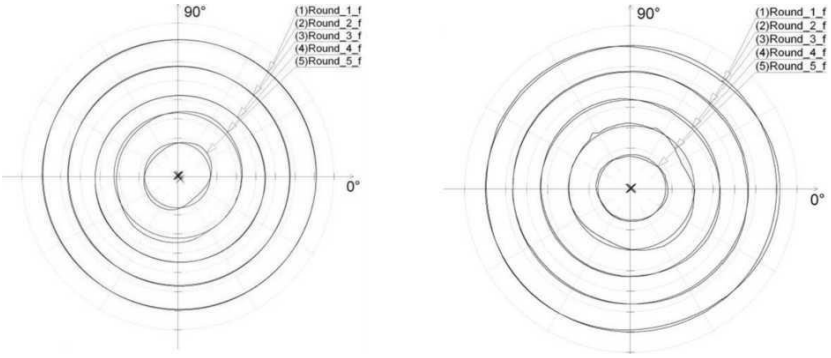

(1) (2)

Fig. 6. Deviations from the roundness of the shaft-swivel part, where: 1 - machining with the use of a tensile force shaft; 2 - without stretching, during standard processing.

The forms of the low-rigid shaft rolling oscillations, obtained during grinding without the tensile system and with the system are shown in Fig. 7. The values obtained are shown in Table 6.

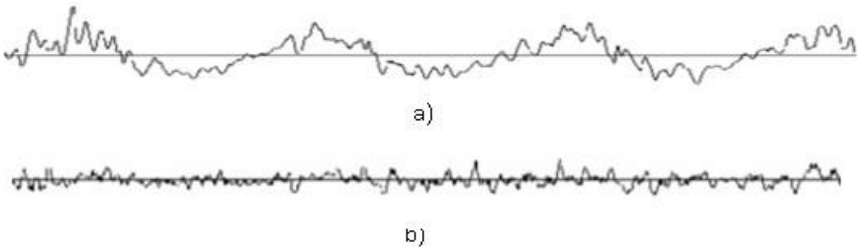

Fig. 7. Oscillogram of the deflection of the machined shaft: without stretching (a), with stretching (b).

Table 6. Deflection of the shaft at machining.

Grinding modes			**Mean value of deflections, µm**	
V_c, m/min	S_f, mm/rev	t, mm	with stretching	without stretching
5.8	15.75	0.005	13.3	200

The experimental data show that for any part point, in particular the processing point directly below the grinder, the size of deflections for low-rigid shafts for the indicated diameter ranges can be substantially reduced through selecting the appropriate tensile force.

The results of the experiments showed that the maximal axis offsetting of the shaft at grinding in the elastically deformed state decreased.

The analysis of the polar-recording charts showed that the deviation from the roundness of the base surface after stretching decreases, but the main thing is that the profilograms show a significant approximation of the detail shape to the cylindrical.

The carried out tests made it possible to establish a decrease in the deviation from the accuracy of the shaft shape compared to standard grinding.

8. Conclusion

The influence of inertia moments and elastic and dissipative forces to changing of in-processing moving shaft were investigated. Changing of TS headstock and tailstock inertia moment influences essentially the in-processing shaft angular velocity and accelerations. The variation of in-processing shaft coefficients of rigidity, viscous resistance and stretching forces were performed to reduce the range of angular velocity and accelerations change. Rigidity increase at the expense of stretching led to reduction of in-processing shaft deformation and reduction of transition process. The amplitude of angular velocity fluctuations is reduced considerably by the increase of in-processing shaft viscous resistance coefficient. It confirms that the amplitude and frequency of in-processing shaft angular velocity and accelerations fluctuations depend on the inertia moment and elastic and dissipative forces. Thus, corresponding meanings of driving moment, stretching

force and cutting forces moments were determined for a set of in-processing shaft inertia moments of rotating masses, rigidity, and viscous resistance coefficients.

By solving the boundary-value problem of the Pontryagin maximum principle, transient processes for the in-process shaft are obtained. As a result, optimal values of constructive and technological parameters were obtained, which ensure uniformity of shaft motion during processing.

Mathematical models are developed for accuracy control of shaft processing and optimization of parameters for longitudinal-transverse bending. The regularities of the change in the elastic axis of the shaft under the action of tensile forces and bending moments are established. The values of tensile forces, bending moments and deflections of the shaft along the sections in process are determined. The developed methods of shaft processing due to the eccentric stretching by longitudinal force and due to the application of the bending moments provide an increase in processing accuracy by an order of magnitude in comparison with the previous developments.

Nomenclatures

a	Coordinate of application of the transverse loading
b_{sh}	Coefficient of viscous resistance of the processed shaft, N·m·s/rad
c_{sh}	Coefficient of processed shaft rigidity, N·m/rad;
e	Eccentricity, m
G, E	shear and elasticity modules of the shaft material, N/m^2
I_p	Polar moment of inertia, m^4
j_1, j_2, j_3	Inertial moments of rotating mass of TS, N·m·s^2
l	Length of the shaft, m
M_d	Driving moments of the processed shaft, N·m
M_g	Driving moments of the grinding wheel, N·m
M_R	Moment of resistance in the process of shaft grinding, N·m
r_{sh}	Radius of the shaft; m.
y_{def}	Elastic deformation, μm

Greek Symbols

ϕ_1, ϕ_2	Angular displacements of TS rotating mass in the processing, rad
$\dot{\phi}_1, \dot{\phi}_2, \dot{\phi}_3$	Angular rates of TS rotating mass in the processing, s^{-1}
$\ddot{\phi}_1, \ddot{\phi}_1, \ddot{\phi}_3$	Angular accelerations of TS rotating mass in the processing, s^{-2};
ω	Frequency of the process, s^{-1}
ψ_1, ψ_2	Auxiliary functions

Abbreviations

MM	Journal of Engineering Science and Technology
TS	International Standard Atmosphere

References

1. Kolokatov, A.M.; Baykalova, V.N.; and Shitov A.N. (2012). *Grinding with the abrasive and diamond tool*. Moscow: MSU Publications.
2. Taranenko, W.; Taranenko, G.; Szabelski, J.; and Swic, A. (2008). Identification of dynamic system of grinding of low rigidity shafts (in Polish). *Modelowanie Inżynierskie*, 4(35), 115-130.
3. Zil, V.V. (1998). *Cutting theory*. Methodical instructions on practical exercises for students of specialties 7.09.02.02. Department of Mining Engineering Technology, Dnepropetrovsk (private communication - in Russian).
4. Macchelli, A.; Secchi, C.; and Van der Schaft, A. (2013). Lagrangian and Hamiltonian methods for modeling and control. *European Journal of Control*. 19(6), 437-530.
5. Azimov, B.M.; and Sulyukova, L.F. (2012). *Mathematic modelling and the optimal control of the small rigidity details processing technological system.* Spravochnik Handbook. Moscow: Spektr Publishing house.
6. Azimov, B.M.; and Sulyukova, L.F. (2017). The calculation and optimal control by the technological processes of a puller shaft turning processing. *American Journal of Science and Technology*, 4(1), 5-12.
7. Salikhov, Z.M.; Sulyukova, L.F.; and Azimov, B.M. (2007). Mathematic modeling and determination of the details processing technological system energetic state. *Uzbek Journal of Informatics and Energetic Problems*, 27(1), 8-13. (private communication - in Russian).
8. Cardi, A.A.; Firpi, H.A.; Bement, M.T.; and Liang, S.Y. (2008). Workpiece dynamic analysis and prediction during chatter of turning process. *Mechanical Systems and Signal Processing*, 22(6), 1481-1494.
9. Swic, A.; Wolos, D.; Zubrzycki, J.; Opielak, M.; Gola, A.; and Taranenko, V. (2014). Accuracy control in the machining of low rigidity shafts. *Applied Mechanics and Materials*, 613, 357-367.
10. Szabelski, J.; Taranenko, V.; Taranenko, G.; and Bagimov, I. (2013). Modelling and systemic analysis of models of dynamic systems of shaft machining. *IFAC Proceedings Volume*, 42(4), 1736-1741.
11. Afanasiev, V.N.; Kolmanovskii, V.; and Nosov, V.R. (1996). *Mathematical theory of control systems design*. Netherlands: Springer.
12. Nocedal, J.; and Wright, S. (2006). *Numerical optimization. Springer Series in Operations Research and Financial Engineering*. London: Springer.
13. Rao, R.V. (2011). Modelling and optimization of machining processes. *Advanced modelling and optimization of manufacturing processes*. London: Springer-Verlag.
14. Vasiliev, F.P. (1988). *Numeric methods of extremal problems solutions*. Moscow: Nauka.